Conformational Preferences of X-Pro Sequences: Ala-Pro and Aib-Pro Motifs

Byung Jin Byun,[†] Il Keun Song,[†] Yong Je Chung,[‡] Keun Ho Ryu,[§] and Young Kee Kang*,[†]

Department of Chemistry, Department of Biochemistry, and Database/Bioinformatics Laboratory, Chungbuk National University, Cheongju, Chungbuk 361-763, Republic of Korea

Received: July 31, 2010; Revised Manuscript Received: September 23, 2010

Conformational preferences and prolyl cis−trans isomerizations of the X-Pro motifs (Ac-X-Pro-NHMe, X = Ala and Aib) are explored using the meta-hybrid functional M06-2X and the double-hybrid functional B2PLYP-D with empirical dispersion corrections in the gas phase and in water, where solvation free energies were calculated using the implicit SMD model. Ac-Ala-Pro-NHMe favors the type VI β-turns in the gas phase and the open conformations in water. The populations of type VI β-turns decrease from 71% in the gas phase to 21% in water, which is reasonably consistent with IR and NMR experimental results on *t*Boc-Ala-Pro-NHMe. However, Ac-Aib-Pro-NHMe prefers the type I β-turns with α-helical structures for both residues in the gas phase and in water, whose populations are estimated to be 66% in both phases. These calculated results may rationalize why most of the peptaibiotics containing the Aib-Pro sequence have a regular α-helical conformation at the N- or C-terminus but a kinked α-helical structure in the middle of the helix. The cis−trans isomerizations of the Ala-Pro and Aib-Pro peptide bonds proceed via the clockwise rotation with the different backbone conformations. The rotational barriers to cis-to-trans isomerization are estimated to be 19.73 kcal/mol for the Ala-Pro tripeptide and 16.64 kcal/mol for the Aib-Pro tripeptide in water, which indicates that the rotational barrier becomes lower by ∼3 kcal/mol for the Aib-Pro peptide bond. The calculated rotational barrier for Ac-Ala-Pro-NHMe is consistent with the observed value of 19.3 kcal/mol for Suc-Ala-Ala-Pro-Phe-pNA from NMR experiments in a buffered solution.

Introduction

It is known that the X-Pro sequence is a structural motif for the formation of a β-turn in peptides and proteins, although its propensity is relatively lower than the Pro-X sequence.[1] From analyses of X-ray protein structures, the cis population is estimated to be ∼6% for the prolyl X-Pro peptide bond.[2] However, it has been reported that the cis−trans isomerization of the X-Pro bond is often involved in the rate-determining steps for folding and refolding of various proteins.[3] The heterogeneity of the unfolded states of proteins is occasionally caused by the prolyl cis−trans isomerization, which leads to multiple pathways for folding or refolding. In addition, the prolyl cis−trans isomerization was suggested to serve as molecular switches or timers[4] in the multiple elastic motion of cardiac PEVK,[4a] in the actomyosin to propel myosin's lever-arm swing,[4b] in a neurotransmitter-gated ion channel,[4c] in the homodimerization of the G protein SRβ in the nucleotide-free state,[4d] in the tetramer formation of stefin B,[4e] and in the assembly of the two domains N1 and N2 in the gene-3-protein of filamentous phage.[4f]

The Ala-Pro and Aib-Pro sequences, where Aib is α-aminoisobutyric acid, can be prototypes for the X-Pro motif with standard and nonstandard residues for X, respectively. Considerable experimental[5−8] and theoretical[1b,9−11] studies have been carried out on the terminally blocked Ala-Pro peptide to explore its conformational preferences, especially the propensity to form a β-turn. By the analysis of IR and NMR spectra of *t*Boc-Ala-Pro-NHMe in various solvents, it was suggested that the Ala-*trans*-Pro peptide adopts a semiopen C_5C_7 conformation in chlorinated solvents, in which the carbonyl oxygen of the Ala residue forms a bifurcated hydrogen bond with both amide hydrogens of the Ala residue and the C-terminal end group.[5] In addition, a βVI-turn stabilized by an intramolecular $i + 3 \rightarrow i$ hydrogen bond was found to occur for the Ala-*cis*-Pro peptide in those solvents. However, these semiopen and β-turn conformations were switched into open conformations having no intramolecular hydrogen bonds in DMSO and water.[5] In the crystal state, the peptides *t*Boc-Ala-Pro-NH*i*Pr[6] and Ac-Ala-Pro-NHMe[8] were found to adopt an open conformation with the trans prolyl peptide bond and the down-puckered pyrrolidine ring. At the HF/6-31G(d) level of theory, the relative stabilities of various β-turn types were calculated to be in the order βVIa > βVIb′ ≈ βVIb > βI for the Ac-Ala-Pro-NHMe in the gas phase.[11] Several experimental[5,12−16] and theoretical[10] works have focused on the cis−trans isomerization for the Ala-Pro peptide bond of short peptides in solution.

Aib is an achiral residue with two methyl groups on the C^α atom and has been known as one of major components of nonribosomally synthesized peptides in microbial sources,[17−20] which are called "peptaibiotics".[19,20] Aib has a strong propensity to form 3_{10}/α-helical conformations[17,18,20] and type I/I′ β-turns in position $i + 1$.[18,20] However, β-strand structures are strongly disallowed because of close contacts of one of two methyl groups with the C═O group of the preceding residue and the N−H group of the following residue.[20] Most peptaibiotics contain the Aib-Pro sequence,[19,20] which has a regular α-helical conformation at the N- or C-terminus[20] but an α-helical structure with a bend in the middle of the helix.[21] In the short peptides of length ≤4 residues, the Aib-Pro sequence adopts a type I β-turn in positions $i + 1$ and $i + 2$ in crystals and in solution.[22−27] However, this motif prefers the 3_{10}/α-helical structure in oligopeptides.[28] The longer peptides with repeating

* To whom correspondence should be addressed. Telephone: +82-43-261-2285. Fax: +82-43-273-8328. E-mail: ykkang@chungbuk.ac.kr.
† Department of Chemistry.
‡ Department of Biochemistry.
§ Database/Bioinformatics Laboratory.

10.1021/jp107200f
Published on Web 10/15/2010

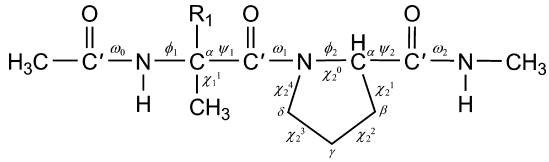

Figure 1. Definition of torsion angles and structural parameters for Ac-X-Pro-NHMe (R_1 = H for Ala and R_1 = CH_3 for Aib).

Aib-Pro sequences form a spiral of β-turns in a ribbon.[29] In addition, the Aib-Pro motif has an α_L-helical/polyproline II (α_L/PP_{II}) conformation in *t*Boc-Aib-Pro-OBzl[30] and an α_R-helical/PP_{II} (α_R/PP_{II}) conformation in *t*Boc-Aib-Pro-Pro-Aib-Val-Ala-Phe-OMe[31] in crystals. Recently, the infrared/UV hole-burning spectroscopy of Z-Aib-Pro-NHMe suggested that its preferred conformation is an α-helical/γ-turn (α_R/C_7^{eq} or α_L/C_7^{eq}) conformation in the gas phase,[32] whereas it is a type I β-turn, i.e., the α_R/α_R conformation, in the crystal[23] and in chloroform.[24] Although considerable theoretical works have been carried out on the conformational preferences of the Aib residue,[33] only a single work reported the preferences of representative conformations for Z-Aib-Pro-NHMe at the B3LYP/6-31+G(d) level of theory in the gas phase to date.[32]

Although there are two theoretical works that focused on the conformational preferences of Ac-Ala-Pro-NHMe[11] and Z-Aib-Pro-NHMe[32] in the gas phase, their preferences were not analyzed utilizing all feasible conformations even in the gas phase. No theoretical works have been carried out to explore the conformational preferences and prolyl cis−trans isomerizations of Ala-Pro and Aib-Pro motifs in water to date. Here, we present the conformational preferences and prolyl cis−trans isomerizations of Ac-Ala-Pro-NHMe and Ac-Aib-Pro-NHMe calculated using dispersion-corrected density functionals with a self-consistent reaction field (SCRF) method in the gas phase and in water. In particular, the conformational preferences are analyzed utilizing all feasible conformations both in the gas phase and in water, which are compared with observed results in solution and in the crystal.

Computational Methods

Chemical structures and torsional parameters for Ac-X-Pro-NHMe (X = Ala and Aib) tripeptides are defined in Figure 1. All Hartree−Fock (HF) and hybrid density functional B3LYP calculations were carried out using the Gaussian 03 package.[34] A recently released Gaussian 09 package[35] was used for the calculations using the meta-hybrid functional M06-2X[36] and the double-hybrid functional B2PLYP-D with empirical dispersion corrections.[37] Here, each backbone conformation of the tripeptides is represented by a capital letter depending on its values of ϕ and ψ for the backbone.[38] Conformations C, E, A, F, and D are equivalent to the γ-turn (C_7^{eq}), extended (C_5), α-helical (α_R), polyproline-like (P_{II} or β), and β_2 structures in the literature, respectively. Conformations A*, C*, D*, and F* are those obtainable by inversion of the ϕ and ψ values of conformations A, C, D, and F, respectively, around the center of the $\phi-\psi$ map. The trans and cis conformations for the X-Pro peptide bond are denoted by "t" and "c", respectively. The down- and up-puckered conformations of the proline ring are defined as those of which the C^γ atom and the C′═O group of the prolyl residue lie on the same and opposite sides, respectively, of the plane defined by the three atoms C^δ, N, and C^α (see Figure 1), which are represented by "d" and "u", respectively. Usually, the down- and up-puckered conformations of the Pro residue have positive and negative values of the endocyclic torsion angle χ^1, respectively. The degree of puckering is described by the puckering amplitude χ_m and the phase angle *P* of Altona and Sundaralingam,[39] where χ_m is the maximum value attainable by endocyclic torsion angles of the ring. Thus, for example, the conformational letter code AtCd for the Ala-Pro tripeptide denotes that the backbone conformation of the Ala residue is A and the backbone conformation of the Pro residue is C with the trans prolyl peptide bond and the down puckering.

The 76 local minima optimized using the ECEPP/3 force field[9] for Ac-Ala-Pro-NHMe, started from the conformations generated by combining local minima of each residue,[9,10] were used as initial points for optimizations at the HF/6-31+G(d) level of theory. All local minima optimized at the HF/6-31G+(d) level of theory were then reoptimized at the B3LYP/6-31+G(d) level of theory and the 35 local minima were obtained. At the B3LYP/6-31+G(d) level of theory, the nine local minima of Ac-Aib-NHMe were identified, which are listed in Table S1 of the Supporting Information, started from the local minima of Ac-Ala-NHMe optimized at the HF/6-31+G(d) level of theory in the gas phase.[40] These nine conformations of Ac-Aib-NHMe and the 10 local minima of Ac-Pro-NHMe optimized at the HF/6-31+G(d) level of theory in the gas phase and in chloroform[40] were combined to provide the initial structures for the Ac-Aib-Pro-NHMe tripeptide using the GaussView program,[41] from which the 47 local minima were identified at the B3LYP/6-31+G(d) level of theory in the gas phase.

Then, all local minima of Ac-Ala-Pro-NHMe and Ac-Aib-Pro-NHMe tripeptides optimized at the B3LYP/6-31+G(d) level of theory were reoptimized at the meta-hybrid functional M06-2X/6-31+G(d) level of theory. In particular, some conformations identified only for Ac-Ala-Pro-NHMe were reoptimized for Ac-Aib-Pro-NHMe and vice versa. In addition, X-ray structures of Ala-Pro-[8] and Aib-Pro-containing[23,26,30,31] peptides were optimized at the same level of theory.

Although we took care of all feasible transition states with the backbone torsion angles ω_1 = +116.4°, +118.0°, −65.1°, and −69.8° as initial structures, as found for the Ac-Pro-NHMe dipeptide,[40] only one transition state ts1 for each of Ac-Ala-Pro-NHMe and Ac-Aib-Pro-NHMe tripeptides with $\omega_1 \approx +120°$ was located after the optimization at the M06-2X/6-31+G(d) level of theory. The most preferred cis conformations FcBd and A*cAd for Ac-Ala-Pro-NHMe and Ac-Aib-Pro-NHMe tripeptides, respectively, were used as starting points for the optimization of transition states. Each transition state was checked by the intrinsic reaction coordinate (IRC) method[42] whether it connects the reactants and products, that is, the trans and cis conformers. However, as in most cases, the IRC calculation did not step all the way to the minimum on either side of the path.[43] Further optimizations were carried out starting from the reactants and products obtained by the IRC method to reach the two minima that the transition state connects.

We used the implicit SMD method[44] implemented in Gaussian 09[35] to compute solvation free energies at the M06-2X/6-31+G(d) level of theory in water. The SMD method is based on the quantum mechanical charge density of a solute molecule interacting with a continuum description of the solvent and was parametrized with a training set of 274 neutral solute and 112 ions in water.[44] The solvation free energy is calculated as the sum of the electrostatic free energy term arising from a SCRF treatment and the cavity-dispersion-solvent-structure free energy term.[44] All local minima and transition states for Ac-Ala-Pro-NHMe and Ac-Aib-Pro-NHMe tripeptides located at the M06-2X/6-31+G(d) level of theory in the gas phase were reoptimized at the SMD M06-2X/6-31+G(d) level of theory in water. Single-

TABLE 1: Torsion Angles and Thermodynamic Properties of Local Minima with $\Delta G < 5$ kcal/mol and Transition State for Ac-Ala-Pro-NHMe Obtained at the B2PLYP-D/6-311++G(d,p)//M06-2X/6-31+G(d) Level of Theory in the Gas Phase

	Ac[a]	Ala[a]			Pro[a]				thermodynamic properties		
conformer[b]	ω_0	ϕ_1	ψ_1	ω_1	ϕ_2	ψ_2	ω_2	χ_2^1	ΔE_e[c]	ΔH[d]	ΔG[e]
FcBd (VIa1)	165.8	−57.7	145.9	8.1	−90.6	13.9	174.6	36.2	0.00	0.00	0.00
DtCd	−173.2	−127.6	80.7	−169.9	−85.6	69.1	−177.7	32.7	2.48	2.61	0.74
EtCd	−178.5	−162.0	156.3	−178.7	−84.2	70.9	−177.3	32.5	0.75	0.21	1.40
EtCu	178.1	−160.8	168.9	−177.9	−83.1	78.7	−175.5	−13.5	2.12	2.35	2.03
FcBu (VIa1)	165.3	−56.0	147.0	6.3	−75.4	−8.7	176.9	−23.2	1.95	1.28	2.06
EcFd (VIb)	177.9	−157.3	156.7	−12.8	−66.0	144.7	−177.2	33.3	4.65	4.62	2.55
EcBd (VIa2)	−178.0	−163.8	154.0	−1.4	−85.2	0.3	177.9	35.1	3.62	2.82	2.79
CtCu	169.2	−67.4	125.7	−178.9	−82.8	78.8	−176.1	−18.5	2.32	2.06	2.90
EcAu (VIa2)	−178.2	−162.3	153.2	−4.1	−68.6	−16.2	179.1	−23.4	4.89	4.82	3.27
DcAd	−174.3	−128.3	52.0	5.3	−95.0	−12.0	178.5	34.6	4.02	3.72	3.69
AtBd (I)	−175.6	−51.9	−37.4	−176.2	−92.5	11.0	176.1	37.9	4.49	4.36	3.94
EtAu	177.3	−161.4	171.0	−176.8	−74.5	−14.9	177.2	−24.2	4.97	4.87	4.31
CtAu	168.0	−65.7	128.7	−177.0	−72.8	−17.1	176.1	−29.0	5.40	5.47	4.41
AtAu (I)	−176.4	−55.5	−31.0	178.7	−68.8	−15.3	179.1	−25.8	4.76	4.67	4.72
AtCd	−178.0	−53.5	−41.8	−174.3	−87.5	70.7	−171.4	35.4	5.73	5.75	4.79
EcFu (VIb)	163.9	−123.6	118.3	−21.0	−49.5	162.3	−179.6	−19.8	4.62	4.68	4.99
ts1	168.0	−59.4	155.8	113.0	−120.9	−2.3	−179.1	29.3	20.79	19.61	18.76

[a] Torsion angles are defined in Figure 1; units in degrees. [b] See the text for definition. For example, the conformational letter code FcBd denotes that the backbone conformations of the Ala residue is F and the backbone conformation of the Pro residue is B with the cis prolyl peptide bond and the down puckering. β-Turn types are shown in parentheses, according to the definition of ref 1e. [c] Relative electronic energies in kcal/mol. [d] Relative enthalpy changes in kcal/mol at 25 °C. [e] Relative Gibbs free energy changes in kcal/mol at 25 °C.

point energies were calculated at the double-hybrid functional B2PLYP-D/6-311++G(d,p) level of theory for all stationary points for both the peptides located at the M06-2X/6-31+G(d) level of theory in the gas phase and at the SMD M06-2X/6-31+G(d) level of theory in water. Recently, the B2PLYP-D/6-311++G(d,p)//SMD M06-2X/6-31+G(d) level of theory provided the populations of backbone and/or prolyl peptide bond for Ac-Ala-NHMe and Ac-Pro-NHMe dipeptides in water that are consistent with observed values.[45]

Vibrational frequencies were calculated for all stationary points of the two tripeptides at both the levels of theory in the gas phase and in water at 25 °C and 1 atm. The scale factor used is 0.9440 that was chosen to reproduce the experimental frequency for the amide I band of *N*-methylacetamide in Ar and N_2 matrixes.[46] The zero-point energy correction and the thermal energy corrections were employed in calculating the Gibbs free energy of each conformation, from which the populations of all local minima were estimated at 25 °C in the gas phase and in water. Each transition state was also confirmed by checking whether it has one imaginary frequency after frequency calculations at both the levels of theory in the gas phase and in water. Here, the ideal gas, rigid rotor, and harmonic oscillator approximations were used for the translational, rotational, and vibrational contributions to the Gibbs free energy, respectively.[47]

Results and Discussion

Ac-Ala-Pro-NHMe. We obtained 44 local minima and one transition state for Ac-Ala-Pro-NHMe at the M06-2X/6-31+G(d) level of theory in the gas phase. The backbone torsion angles and thermodynamic properties of 16 local minima with relative Gibbs free energy $\Delta G < 5$ kcal/mol and the transition state ts1 at the B2PLYP-D/6-311++G(d,p)//M06-2X/6-31+G(d) level of theory in the gas phase are listed in Table 1. The torsion angles for side chains and the puckering parameters for the prolyl ring of these conformations are presented in Table S2 of the Supporting Information. The corresponding values for other local minima with $\Delta G > 5$ kcal/mol are listed in Tables S3 and S4 of the Supporting Information, respectively.

In the gas phase, the most preferred conformation of the Ala-Pro tripeptide is FcBd with a type VIa1 β-turn (or $\beta\alpha_R$ in Ramachandran nomenclature),[1e] which is shown in Figure S1a of the Supporting Information. This conformation FcBd has the PP_{II} structure for the Ala residue and the 3_{10}-helical structure with the cis prolyl peptide bond and the down puckering for the Pro residue, in which the C_{10} hydrogen bond between the carbonyl oxygen of the acetyl group and the amide hydrogen of the C-terminal NHMe group with a distance of $d(C{=}O_{Ac}\cdots H{-}N_{NHMe}) = 1.99$ Å seems to play a role.

The second to fourth preferred conformations are DtCd (Figure S1b of the Supporting Information), EtCd, and EtCu having the trans prolyl peptide bond with $\Delta G = 0.74$, 1.40, and 2.03 kcal/mol, respectively, in the gas phase. The C_7 hydrogen bonds between the carbonyl oxygen of the Ala residue and the amide hydrogen of the C-terminal NHMe group with distances of $d(C{=}O_{Ala}\cdots H{-}N_{NHMe}) = 2.00$, 2.02, and 2.02 Å, respectively, appear to be responsible in stabilizing these local minima. By the analysis of IR and NMR spectra of *t*Boc-Ala-Pro-NHMe, it was suggested that the most feasible conformation adopts a semiopen C_5C_7 (i.e., EtCd or EtCu) conformation in chlorinated solvents.[5]

We identified only one transition state ts1 for the cis−trans isomerization of the Ala-Pro peptide bond with $\omega_1 = +113.0°$ in the gas phase, whereas the clockwise and anticlockwise rotations through $\omega_1 \approx +120°$ and $-60°$, respectively, are feasible for the Ac-Pro peptide bond of Ac-Pro-NHMe.[40] This transition state ts1 has a hydrogen bond between the prolyl nitrogen and the following N−H group with the distance of $d(N_{Pro}\cdots H{-}N_{NHMe}) = 2.18$ Å (see Figure S1e of the Supporting Information) that plays a role in stabilizing the transition states of Ac-Pro-NHMe.[40]

The 47 local minima and one transition state were obtained for Ac-Ala-Pro-NHMe at the SMD M06-2X/6-31+G(d) level of theory in water. Table 2 lists the backbone torsion angles and thermodynamic properties of 25 local minima with $\Delta G < 5$ kcal/mol and the transition state ts1 at the B2PLYP-D/6-311++G(d,p)//SMD M06-2X/6-31+G(d) level of theory in water. The torsion angles for side chains and the puckering

TABLE 2: Torsion Angles and Thermodynamic Properties of Local Minima with $\Delta G < 5$ kcal/mol and Transition State for Ac-Ala-Pro-NHMe Obtained at the B2PLYP-D/6-311++G(d,p)//SMD M06-2X/6-31+G(d) Level of Theory in Water

	Ac[a]	Ala[a]			Pro[a]				thermodynamic properties		
conformer[b]	ω_0	ϕ_1	ψ_1	ω_1	ϕ_2	ψ_2	ω_2	$\chi_2{}^1$	ΔE_e[c]	ΔH[d]	ΔG[e]
FtFu	176.7	−60.2	150.2	167.3	−51.2	147.1	175.8	−26.2	0.43	0.67	0.00
EtAd	−178.6	−159.8	153.9	174.8	−71.1	−18.6	−179.9	29.6	1.73	1.61	0.06
FcBd (VIa1)	175.5	−54.6	144.9	5.1	−88.5	11.0	174.4	37.0	0.00	0.00	0.48
EtFu	−179.4	−159.6	157.5	169.9	−53.0	146.2	178.1	−25.6	1.66	1.74	0.55
AtFu	175.7	−56.7	−39.4	−179.5	−56.3	145.0	175.3	−28.0	1.21	1.42	0.71
FtAu	176.1	−61.4	153.1	170.9	−60.6	−27.6	−177.2	−23.1	1.34	1.64	1.19
EcAd (VIa2)	−179.1	−159.4	148.8	−3.1	−78.3	−10.5	−179.4	34.3	1.99	1.88	1.20
EcFd (VIb)	−178.7	−159.3	155.0	−11.7	−68.1	163.8	176.9	35.3	1.98	2.09	1.22
EtAu	−177.3	−162.0	166.3	175.2	−67.1	−21.1	−178.1	−20.7	2.47	1.73	1.49
EcFu (VIb)	−178.1	−161.4	153.9	−17.1	−55.3	162.9	176.8	−22.7	2.72	2.67	1.61
AtAu (I)	178.0	−52.7	−35.9	178.7	−64.8	−18.7	−177.7	−23.4	0.56	0.79	1.66
AtBd (I)	178.4	−49.7	−42.0	−176.2	−86.3	3.0	179.7	36.5	1.56	1.51	1.72
AtFd	173.7	−54.9	−53.6	−179.5	−65.3	148.4	176.9	28.7	2.70	2.99	1.91
A*tFd	−176.1	47.5	50.8	177.7	−60.7	145.4	175.7	27.1	2.43	2.56	2.16
EcAu (VIa2)	−178.2	−158.4	149.6	−8.9	−67.1	−19.5	−176.6	−19.8	3.26	3.26	2.45
FcBu (VIa1)	176.5	−54.5	146.8	1.7	−73.5	−7.7	175.5	−24.1	1.67	1.86	2.50
DcAd	−177.7	−129.0	59.3	3.5	−93.4	−10.2	−178.8	36.0	2.41	2.39	2.77
DtAd	−179.8	−125.9	62.5	−179.6	−67.4	−22.4	−179.3	29.8	3.03	3.12	2.80
EtCd	−178.4	−160.7	153.3	−178.5	−85.0	59.5	179.4	34.8	3.33	3.43	3.06
A*cAd	174.9	53.8	54.0	7.6	−98.0	−12.1	−175.3	36.0	2.22	2.35	3.66
F*cBd	−177.2	77.8	150.6	−5.6	−84.4	−3.1	−178.6	36.6	5.40	5.55	3.70
A*cFd	176.8	52.2	55.9	4.0	−92.9	161.5	173.2	36.8	2.28	1.86	4.28
AtCd	175.4	−56.7	−43.0	−171.1	−89.2	62.4	−177.3	35.9	4.12	4.28	4.29
F*tAu (II′)	−177.6	70.0	176.0	177.5	−66.0	−21.7	−178.3	−24.2	4.98	5.08	4.43
GtFd	−179.7	−150.7	−78.1	174.7	−58.9	148.5	175.4	28.6	5.87	6.25	4.88
ts1	179.5	−59.9	153.5	117.5	−126.0	1.0	178.1	32.1	21.57	20.34	20.21

[a] Torsion angles are defined in Figure 1; units in degrees. [b] See the text for definition. For example, the conformational letter code FcBd denotes that the backbone conformations of the Ala residue is F and the backbone conformation of the Pro residue is B with the cis prolyl peptide bond and the down puckering. β-Turn types are shown in parentheses, according to the definition of ref 1e. [c] Relative electronic energies in kcal/mol. [d] Relative enthalpy changes in kcal/mol at 25 °C. [e] Relative Gibbs free energy changes in kcal/mol at 25 °C.

parameters for the prolyl ring of these conformations are presented in Table S5 of the Supporting Information. The corresponding values for other local minima with $\Delta G > 5$ kcal/mol are listed in Tables S6 and S7 of the Supporting Information, respectively.

In water, the open conformations FtFu and EtAd with the trans prolyl peptide bond become most preferred and more stabilized by 0.48 and 0.42 kcal/mol in ΔG, respectively, than the most preferred conformation FcBd with a type VIa1 β-turn in the gas phase. These conformations FtFu, EtAd, and FcBd are represented in Figure 2. In particular, the conformation FtFu has the PP_{II} structures for both Ala and Pro residues, as found for Ac-Ala-NHMe and Ac-Pro-NHMe in water.[40] In addition, these first two preferred conformations FtFu and EtAd are more stable by 2.80 and 2.32 kcal/mol in ΔG, respectively, than the trans conformation DtAd, optimized from the second preferred conformation DtCd with $\Delta G = 0.74$ kcal/mol in the gas phase. On the basis of IR and NMR experiments, the open conformations having no intramolecular hydrogen bonds were suggested to be preferentially populated for *t*Boc-Ala-Pro-NHMe in water,[5] which are consistent with the most preferred conformations FtFu and EtAd for the Ala-Pro tripeptide in water.

The conformations AtAu and AtBd with the type I β-turns are found to have ΔG values of 1.66 and 1.72 kcal/mol, respectively, in water, whereas they are more decreased in the magnitude of ΔG of 4.72 and 3.94 kcal/mol, respectively, in the gas phase. However, they still have the C_{10} hydrogen bonds between the acetyl group and the C-terminal NHMe group with distances of $d(C{=}O_{Ac}\cdots H{-}N_{NHMe}) = 1.98$ and 2.02 Å, respectively, in water, which are similar to those in the gas phase. The transition state ts1 for the cis−trans isomerization of the Ala-Pro peptide bond is located at $\omega_1 = +117.5°$ in water, which is similar to that in the gas phase. The overall conformations of ts1 are almost the same in water and in the gas phase (see Figure 2d and Figure S1e of the Supporting Information). In particular, the hydrogen bond between the prolyl nitrogen and the following N−H group of the ts1 still survives in water and its distance $d(N_{Pro}\cdots H{-}N_{NHMe})$ is 2.19 Å.

Ac-Aib-Pro-NHMe. The 55 local minima and one transition state were obtained for Ac-Aib-Pro-NHMe at the M06-2X/6-31+G(d) level of theory in the gas phase. The backbone torsion angles and thermodynamic properties of 34 local minima with $\Delta G < 5$ kcal/mol and the transition state ts1 at the B2PLYP-D/6-311++G(d,p)//M06-2X/6-31+G(d) level of theory in the gas phase are listed in Table 3. The torsion angles for side chains and the puckering parameters for the prolyl ring of these conformations are presented in Table S8 of the Supporting Information. The corresponding values for other local minima with $\Delta G > 5$ kcal/mol are listed in Tables S9 and S10 of the Supporting Information, respectively.

In the gas phase, the most preferred conformation of the Aib-Pro tripeptide is AtAu, followed by the conformation AtBd with $\Delta G = 0.22$ kcal/mol. These two conformations have in common the type I β-turns with the C_{10} hydrogen bonds between the acetyl group and the C-terminal NHMe group having the distances of $d(C{=}O_{Ac}\cdots H{-}N_{NHMe}) = 1.98$ and 2.01 Å, respectively, which are shown in Figures S2a,b of the Supporting Information, respectively. For the Ala-Pro tripeptide, these β-turn structures are less stable by 4.72 and 3.94 kcal/mol, respectively, in ΔG than the most preferred conformation FcBd with a type VIa1 β-turn, as noted above. In the case of the Aib-Pro tripeptide, the conformation FcBd, however, has $\Delta G = 1.87$ kcal/mol and a little longer distance of 2.06 Å for the C_{10} hydrogen bond between the acetyl group and the C-terminal

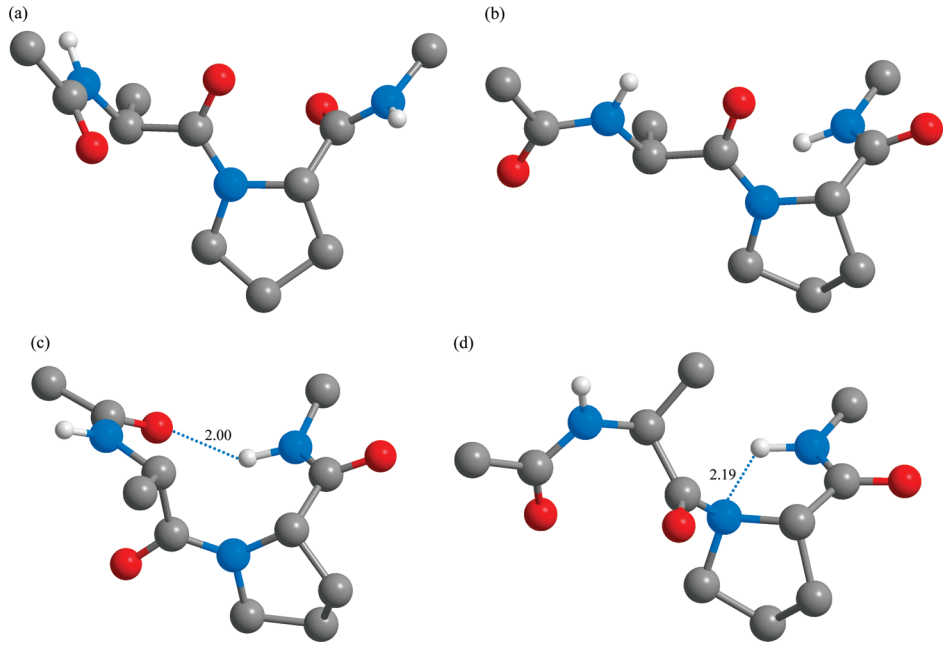

Figure 2. Representative local minima and transition state ts1 for Ac-Ala-Pro-NHMe obtained at the B2PLYP-D/6-311++G(d,p)//SMD M06-2X/6-31+G(d) level in water: local minima (a) FtFu (0.00), (b) EtAd (0.06), (c) FcBd (0.48), and (d) transition state ts1 (20.21), where ΔG (kcal/mol) are shown in parentheses. Hydrogen bonds are represented by broken lines and the corresponding distances (Å) are also shown.

NHMe group than that of the Ala-Pro tripeptide. In particular, the close contacts of the second methyl group substituted at the C^{α} carbon of the Aib residue with the amide nitrogen, C^{α}, and carbonyl carbon of the Pro residue, whose distances are 3.13, 3.07, and 3.15 Å, respectively, appear to be responsible in destabilizing this conformation FcBd (see Figure S2c of the Supporting Information). IR studies of Z-Aib-Pro-NHMe showed that this tripeptide exhibits a strong tendency to form the type I β-turn in chloroform.[24]

The third preferred conformation is A*cAd (Figure S2d of the Supporting Information) having the cis prolyl peptide bond and its ΔG is 0.85 kcal/mol in the gas phase, in which there is a C_{10} hydrogen bond between the acetyl group and the C-terminal NHMe group with the distance of $d(C{=}O_{Ac}\cdots H{-}N_{NHMe}) = 2.48$ Å, as found for the β-turn structures AtAu, AtBd, and FcBd. The fourth and sixth preferred conformations are AtCd and A*tCd with $\Delta G = 0.98$ and 1.51 kcal/mol in the gas phase, respectively. The C_7 hydrogen bonds between the carbonyl oxygen of the Aib residue and the amide hydrogen of the C-terminal NHMe group with distances of $d(C{=}O_{Aib}\cdots H{-}N_{NHMe}) = 2.07$ and 1.96 Å, respectively, appear to be responsible in stabilizing these local minima. These conformations AtCd and A*tCd are shown in Figures S2e,f of the Supporting Information. Recently, the infrared/UV hole-burning spectroscopy of Z-Aib-Pro-NHMe suggested that its preferred conformations are A*tCd and AtCd in the gas phase.[32]

As found for the Ala-Pro tripeptide, only one transition state ts1 was located for the cis−trans isomerization of the Aib-Pro peptide bond with $\omega_1 = +122.6°$ in the gas phase. This transition state ts1 has also a hydrogen bond between the prolyl nitrogen and the following N−H group with the distance of $d(N_{Pro}\cdots H{-}N_{NHMe}) = 2.13$ Å (Figure S2g of the Supporting Information), as seen for the Ala-Pro tripeptide and Ac-Pro-NHMe.[40] However, the backbone structure of the ts1 for the Aib-Pro peptide is different from that for the Ala-Pro peptide because of the different starting structures used for optimization, as described above.

We obtained the 56 local minima and one transition state for Ac-Aib-Pro-NHMe at the SMD M06-2X/6-31+G(d) level of theory in water. Table 4 lists the backbone torsion angles and thermodynamic properties of 17 local minima with $\Delta G < 5$ kcal/mol and the transition state ts1 at the B2PLYP-D/6-311++G(d,p)//SMD M06-2X/6-31+G(d) level of theory in water. The torsion angles for side chains and the puckering parameters for the prolyl ring of these conformations are presented in Table S11 of the Supporting Information. The corresponding values for other local minima with $\Delta G > 5$ kcal/mol are listed in Tables S12 and S13 of the Supporting Information, respectively.

In water, the most preferred conformation of the Aib-Pro tripeptide is AtAu, as found in the gas phase, and followed by the conformation A*tFd with $\Delta G = 0.43$ kcal/mol. The conformation AtAu has a type I β-turn with the C_{10} hydrogen bond between the acetyl group and the C-terminal NHMe group having the distance of $d(C{=}O_{Ac}\cdots H{-}N_{NHMe}) = 1.95$ Å (Figure 3a). The conformation A*tFd has the α_L-helical structure for the Aib residue and the down-puckered PP_{II} structure for the Pro residue (Figure 3b), which is not a local minimum in the gas phase (see Tables 3 and S9 of the Supporting Information) but found as a preferred conformation of *t*Boc-Aib-Pro-OBzl in the crystal.[30] The third and fourth preferred conformations are AtBd and AtFd with trans prolyl peptide bond in water, whose ΔG are 0.83 and 1.26 kcal/mol, respectively. The conformation AtBd has also a type I β-turn with the distance of $d(C{=}O_{Ac}\cdots H{-}N_{NHMe}) = 1.99$ Å. The conformation AtFd has the α_R-helical structure for the Aib residue and the down-puckered PP_{II} structure for the Pro residue, which is found as a preferred conformation for the Aib-Pro sequence of *t*Boc-Aib-Pro-Pro-Aib-Val-Ala-Phe-OMe in the crystal.[31]

The most preferred conformations for the Aib-*cis*-Pro tripeptide are A*cBd and A*cFd with $\Delta G = 3.03$ and 3.04 kcal/mol, respectively, in water, whereas the value of ΔG for the corresponding conformation A*cAd is 0.85 kcal/mol in the gas phase (see Table 3). In particular, a weak C_{10} hydrogen bond between the acetyl group and the C-terminal NHMe group with the distance of $d(C{=}O_{Ac}\cdots H{-}N_{NHMe}) = 2.63$ Å is likely to contribute to stabilizing the conformation A*cBd (Figure 3c). Although the PP_{II} structure FtFu is most preferred for the Ala-Pro tripeptide in water (see Table 2),

TABLE 3: Torsion Angles and Thermodynamic Properties of Local Minima with $\Delta G < 5$ kcal/mol and Transition State for Ac-Aib-Pro-NHMe Obtained at the B2PLYP-D/6-311++G(d,p)//M06-2X/6-31+G(d) Level of Theory in the Gas Phase

	Ac[a]	Aib[a]			Pro[a]				thermodynamic properties		
conformer[b]	ω_0	ϕ_1	ψ_1	ω_1	ϕ_2	ψ_2	ω_2	χ_2^1	ΔE_e[c]	ΔH[d]	ΔG[e]
AtAu (I)	−173.7	−53.0	−34.9	−178.3	−67.3	−16.5	179.3	−24.3	0.34	0.72	0.00
AtBd (I)	−172.2	−51.2	−40.5	−173.3	−90.1	9.2	176.2	38.2	0.13	0.00	0.22
A*cAd	172.7	64.1	38.3	8.0	−97.0	−14.5	177.2	35.2	0.00	0.46	0.85
AtCd	−175.3	−49.2	−45.8	−179.0	−87.0	73.3	−167.4	35.9	1.54	2.17	0.98
F*tCd	−164.0	53.7	−157.6	−174.1	−88.4	62.4	−174.0	36.0	3.55	4.21	1.37
A*tCd	172.5	52.2	44.3	179.4	−84.1	74.7	−177.6	33.1	1.64	2.20	1.51
EtCu	177.7	−177.9	−172.9	−175.8	−83.3	83.7	−174.4	−9.0	2.59	3.45	1.82
A*tCu	175.8	44.7	51.6	−171.2	−89.2	77.3	−175.7	−10.3	3.10	3.62	1.84
FcBd (VIa1)	166.1	−51.8	141.0	7.8	−86.8	−4.7	173.5	35.3	1.71	2.32	1.87
E*tCd	−176.7	174.8	172.5	178.1	−83.4	74.3	−177.2	33.1	1.65	2.49	1.97
F*tBd (II′)	−167.8	51.3	−134.2	−175.2	−78.4	−2.3	176.7	37.2	1.86	2.79	2.49
DcBd	−174.5	−171.0	39.2	8.9	−97.5	−4.3	−172.5	35.4	4.80	5.18	2.55
D*tCd (IV)	172.4	174.8	−52.6	178.9	−82.5	76.7	−177.8	30.1	4.53	5.14	2.80
E*cBd	−176.4	175.4	170.5	−0.8	−90.5	−9.8	175.4	36.3	3.61	4.19	2.90
A*cAu	170.4	65.5	40.3	4.8	−90.1	−21.6	178.8	−15.7	2.42	2.92	2.99
CtCd	168.5	−53.6	123.3	−175.8	−89.0	73.9	−177.0	31.5	3.15	4.05	3.14
F*tAu (II′)	−164.5	54.2	−147.3	176.7	−67.7	−11.5	177.1	−29.0	2.91	3.64	3.27
AcAu	−174.2	−67.5	−18.3	5.1	−62.8	−33.0	−175.8	−30.6	4.30	4.76	3.42
AcAd	−172.4	−70.7	−24.5	25.6	−80.5	−26.7	179.4	25.0	4.01	4.52	3.43
E*tBd	−177.0	174.8	173.2	179.0	−80.4	−4.9	174.9	32.0	4.22	4.87	3.69
DtCd	−171.1	−174.3	57.1	−169.8	−87.4	69.0	−178.2	37.0	5.35	6.10	3.71
D*tFd	173.4	177.7	−60.6	155.8	−56.9	150.6	−177.4	31.0	4.25	4.90	3.76
FcAu (VIa1)	165.4	−52.8	148.4	−4.4	−71.1	−15.2	175.6	−21.9	4.16	4.59	3.84
F*tCu	−163.6	54.0	−155.9	172.8	−81.7	77.3	−168.6	−12.1	4.45	5.13	3.90
CtCu	169.2	−52.3	129.4	170.8	−81.1	83.0	−175.7	−25.2	3.97	4.93	4.11
C*tCd (V′)	−168.9	56.7	−118.5	−174.4	−82.5	68.4	−176.0	38.3	3.79	4.04	4.30
EtAu	176.5	−177.4	−167.5	−175.5	−69.5	−19.4	176.9	−24.5	5.24	5.91	4.37
DtCu	−167.7	−122.1	67.2	−173.4	−84.8	79.2	−175.1	−11.8	5.50	6.32	4.46
C*cBd	−169.7	51.8	−126.7	30.4	−103.8	−8.6	178.6	33.5	4.93	5.45	4.48
DtCu	−170.6	−176.1	56.3	−176.0	−83.9	80.3	−174.6	−5.3	5.10	5.19	4.54
D*tCu (IV)	173.4	117.0	−40.5	−178.3	−79.6	86.7	−175.1	−18.4	4.58	4.71	4.70
DcFd	−171.4	−168.2	41.6	10.8	−91.3	166.3	175.0	36.1	5.21	5.73	4.70
D*cBd	171.4	177.0	−55.7	−5.3	−92.1	−3.9	175.4	38.3	6.93	7.30	4.80
AcFd	−165.7	−75.9	−18.6	22.3	−76.6	163.7	175.3	29.6	6.41	6.99	4.91
ts1	175.4	56.2	40.8	122.6	−128.2	2.4	−179.3	34.2	16.87	16.41	15.91

[a] Torsion angles are defined in Figure 1; units in degrees. [b] See the text for definition. For example, the conformational letter code FcBd denotes that the backbone conformations of the Aib residue is F and the backbone conformation of the Pro residue is B with the cis prolyl peptide bond and the down puckering. β-Turn types are shown in parentheses, according to the definition of ref 1e. [c] Relative electronic energies in kcal/mol. [d] Relative enthalpy changes in kcal/mol at 25 °C. [e] Relative Gibbs free energy changes in kcal/mol at 25 °C.

this conformation becomes remarkably unstable for the Aib-Pro tripeptide in water, whose ΔG is 4.76 kcal/mol (Table 4). In addition, the conformation FcBd with a type VIa1 β-turn is most preferred for the Ala-*cis*-Pro tripeptide and its ΔG is 0.48 kcal/mol in water, but this structure is not quite feasible for the Aib-Pro tripeptide in water because its ΔG is 5.96 kcal/mol (see Table S12).

The transition state ts1 for the cis−trans isomerization of the Aib-Pro peptide bond is located at $\omega_1 = +118.5°$ in water, which is similar to that in the gas phase. The overall conformations of ts1 are almost the same both in water and in the gas phase (see Figures 3d and S2g of the Supporting Information). In particular, the hydrogen bond between the prolyl nitrogen and the following N−H group of the ts1 is still survived in water and its distance $d(N_{Pro}\cdots H{-}N_{NHMe})$ is 2.18 Å. As found in the gas phase, ts1 of the Aib-Pro tripeptide has the backbone torsion angles different from those of ts1 of the Ala-Pro tripeptide in water, which is ascribed to the different starting structures used for optimization of Aib-Pro and Ala-Pro tripeptides, as described above.

Population of β-Turns. For the Ala-Pro tripeptide, the populations of β-turns with types VIa1, VIb, VIa2, and I are obtained to be 69.5, 0.9, 0.9, and 0.1% in the gas phase, respectively, and 12.0, 5.0, 3.8, and 3.0% in water, respectively, where the conformation FcBd contributes significantly to the population of the type VIa1, as described above. The decrease of the total population for VI β-turns from 71.3% in the gas phase to 20.9% in water is reasonably consistent with IR and NMR experimental results on *t*Boc-Ala-Pro-NHMe,[5] which suggested that the type VI β-turn was found to occur in chlorinated solvents and they were switched into open conformations having no intramolecular hydrogen bonds in water.

The relative stabilities of β-turns were calculated to be in the order VIa1 (0.0) > VIb (2.1) > I (2.9) > VIa2 (3.2) for Ac-Ala-Pro-NHMe, where the values in parentheses are relative energies in kcal/mol calculated at the MP2/6-31G(d)//HF/6-31G(d) level of theory in the gas phase[11] and the types VIa1, VIb, and VIa2 are designated as VIa, VIb′, and VIb in ref 11, respectively. However, the relative stabilities of β-turns for Ac-Ala-Pro-NHMe are calculated to be in the orders VIa1 > VIa2 > I > VIb by ΔE with 0.00, 3.62, 4.49, and 4.65 kcal/mol, respectively, and VIa1 > VIb > VIa2 > I by ΔG with 0.00, 3.62, 4.49, and 4.65 kcal/mol, respectively, at the B2PLYP-D/6-311++G(d,p)//M06-2X/6-31+G(d) level of theory in the gas phase. In water, the relative stabilities of β-turns are estimated to be in the order VIa1 (FcBd) > VIa2 (EcAd) ≈ VIb (EcFd) > I (AtAu) by $\Delta\Delta G$ with 0.00, 0.72, 0.74, and 1.17 kcal/mol,

TABLE 4: Torsion Angles and Thermodynamic Properties of Local Minima with $\Delta G < 5$ kcal/mol and Transition State for Ac-Aib-Pro-NHMe Obtained at the B2PLYP-D/6-311++G(d,p)//SMD M06-2X/6-31+G(d) Level of Theory in Water

	Ac[a]	Aib[a]			Pro[a]				thermodynamic properties		
conformer[b]	ω_0	ϕ_1	ψ_1	ω_1	ϕ_2	ψ_2	ω_2	χ_2^1	ΔE_e[c]	ΔH[d]	ΔG[e]
AtAu (I)	179.2	−49.4	−38.4	−178.6	−63.0	−21.5	−178.9	−23.5	0.00	0.00	0.00
A*tFd	−179.1	50.3	40.8	175.2	−62.4	148.3	174.9	27.6	1.52	1.52	0.43
AtBd (I)	−177.9	−48.7	−43.6	−173.3	−83.2	−0.4	177.8	35.9	1.03	0.97	0.83
AtFd	178.3	−48.0	−54.2	−175.8	−62.9	146.4	174.7	26.1	2.64	2.56	1.26
A*tCd	178.7	49.2	47.6	178.3	−83.8	62.2	−180.0	34.6	4.21	4.00	2.86
A*cBd	173.9	61.5	45.8	1.9	−96.2	−8.3	179.6	38.0	2.39	2.29	3.03
A*cFd	173.4	58.2	46.1	2.7	−95.3	163.8	174.0	38.5	2.53	2.66	3.04
FtAd	175.4	−60.9	164.8	174.7	−68.3	−19.9	179.6	31.6	4.58	4.62	3.24
F*tFu	−176.6	59.8	−159.4	179.6	−56.6	144.3	177.9	−30.2	4.00	4.02	3.33
AcFd	−177.5	−55.2	−40.8	17.8	−78.6	139.6	177.5	29.0	4.74	4.90	3.49
AtCd	−179.7	−51.7	−44.0	−168.1	−88.8	65.8	−177.3	36.4	4.18	3.97	3.57
F*tBd (II′)	179.5	53.9	−131.6	−174.3	−71.7	−8.5	178.5	35.5	3.96	4.26	4.14
AtCu	179.0	−46.8	−43.9	173.2	−75.6	95.4	−172.0	−5.1	3.97	4.13	4.45
FtFu	178.0	−53.8	145.2	167.3	−54.6	147.7	177.1	−30.9	5.22	5.32	4.76
D*tFu	179.3	115.6	−43.0	−177.9	−59.2	146.8	175.2	−29.3	6.33	6.24	4.81
A*tCu	−178.1	44.0	56.3	−171.5	−88.2	75.4	−175.3	−11.3	5.30	5.22	4.81
F*tAu (II′)	−177.9	56.8	−148.2	176.9	−64.3	−13.6	179.2	−29.8	4.08	3.80	4.83
ts1	−175.6	51.3	45.5	118.5	−128.0	−1.2	178.6	33.8	20.15	18.85	19.67

[a] Torsion angles are defined in Figure 1; units in degrees. [b] See the text for definition. For example, the conformational letter code FcBd denotes that the backbone conformations of the Aib residue is F and the backbone conformation of the Pro residue is B with the cis prolyl peptide bond and the down puckering. β-Turn types are shown in parentheses, according to the definition of ref 1e. [c] Relative electronic energies in kcal/mol. [d] Relative enthalpy changes in kcal/mol at 25 °C. [e] Relative Gibbs free energy changes in kcal/mol at 25 °C.

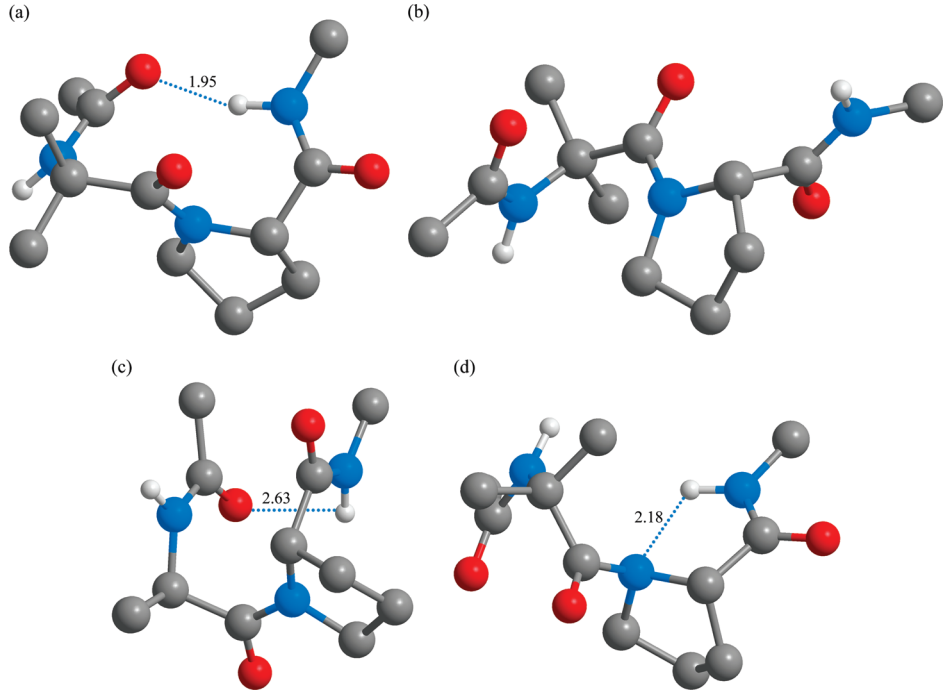

Figure 3. Representative local minima and transition state ts1 for Ac-Aib-Pro-NHMe obtained at the B2PLYP-D/6-311++G(d,p)//SMD M06-2X/6-31+G(d) level in water: local minima (a) AtAu (0.00), (b) A*tFd (0.43), (c) A*cBd (3.03), and (d) transition state ts1 (19.67), where ΔG (kcal/mol) are shown in parentheses. Hydrogen bonds are represented by broken lines and the corresponding distances (Å) are also shown.

respectively, at the B2PLYP-D/6-311++G(d,p)//SMD M06-2X/6-31+G(d) level of theory.

For the Aib-Pro tripeptide, the populations of β-turns are obtained to be 66.4, 1.7, 0.8, and 0.4% for types I, VIa1, II′, and IV, respectively, in the gas phase and the populations are computed to be 66.1 and 0.1% for types I and II′, respectively, in water. This indicates the type I β-turns are preferentially favored for the Aib-Pro tripeptide both in the gas phase and in water. The conformations AtAu and AtBd dominantly contribute to the populations of the type I β-turns, whose populations are 39.4 and 27.0% in the gas phase, respectively, and 53.1 and 13.1% in water, respectively. It has been reported that Z-Aib-Pro-NHMe exhibits a strong tendency to form the type I β-turn in chloroform[24] and in the crystal,[23] and Ac-Aib-Pro-NH*i*Pr forms also a type I β-turn in the crystal.[26]

Comparison with X-ray Structures. In the crystal state, the *t*Boc-Ala-Pro-NH*i*Pr[6] and Ac-Ala-Pro-NHMe[8] tripeptides were found to adopt an open conformation with the trans prolyl peptide bond and the down-puckered pyrrolidine ring, i.e., the conformation DtAd. This conformation DtAd was converged to the conformation DtCd with $\Delta G = 0.74$ kcal/mol after optimization at the M06-2X/6-31+G(d) level of theory in the

gas phase (Table 1). Although its converged structure at the B2PLYP-D/6-311++G(d,p)//SMD M06-2X/6-31+G(d) level of theory in water is quite similar to that in the crystal, its relative free energy ΔG is 2.80 kcal/mol to the most preferred PP_{II} structure FtFu (Table 2).

X-ray structures of the peptides Z-Aib-Pro-NHMe[23] and Ac-Aib-Pro-NH*i*Pr[26] have conformations AtAu and AtBx with type I β-turns, respectively, where x = $E_5/{}^1T_5$ and $E_3/{}^3T_4$ (represented as $E_1/{}^2T_1$ in ref 26). Here, the puckering structures $E_5/{}^1T_5$ and $E_3/{}^3T_4$ denote the intermediates between E_5 (envelope at C^δ) and ${}^1T_5$ (twist; N-exo, C^δ-endo) and between E_3 (envelope at C^β) and ${}^3T_4$ (twist; C^β-exo, C^γ-endo), respectively.[26] The puckering amplitude χ_m and the phase angle P of Altona and Sundaralingam[39] are calculated to be 19.0° and 62.7° for the $E_5/{}^1T_5$ structure, respectively, and 35.1° and 174.4° for the $E_3/{}^3T_4$ structure, respectively. The puckering parameters of the $E_3/{}^3T_4$ structure are quite similar to the χ_m and P values of 38.1° and 161.4° for the conformation AtBd for Ac-Aib-Pro-NHMe optimized at the SMD M06-2X/6-31+G(d) level of theory in water, respectively (see Table S11 of the Supporting Information). The conformation AtAu is found to be preferentially favored for Ac-Aib-Pro-NHMe both in the gas phase and in water, as described above. The conformation AtBd is located as the second and third preferred ones in the gas phase and in water, respectively. However, the intermediate puckerings between the envelope and twist forms are not found for the Pro residue of Ac-Aib-Pro-NHMe either in the gas phase or in water and only the down-puckered structure is favored. The differences in the backbone and pyrrolidine ring conformations for the calculated preferred structures and the observed X-ray structures might be ascribed to the different end groups and the crystal packing that is governed by van der Waals contacts and intermolecular hydrogen bonds.

Population of Cis Prolyl Peptide Bond. The cis populations of the X-Pro peptide bond are computed to be 21.2 and 0.8% for Ala-Pro and Aib-Pro tripeptides, respectively, at the B2PLYP-D/6-311++G(d,p)//SMD M06-2X/6-31+G(d) level of theory in water, which are ascribed to the conformation FcBd with a type VIa1 β-turn and the conformations A*cBd and A*cFd, respectively, as described above. The lower cis population for the Aib-Pro tripeptide is caused by the preferential formation of the conformations AtAu and AtBd with type I β-turns, as described above. The calculated cis population of 21.2% for the Ala-Pro tripeptide is similar to the calculated value of 28%[40] and the observed values of 24 ± 4%[48] and 27 ± 3%[49] for Ac-Pro-NHMe in water. However, it is larger than the experimentally estimated values of 12% for *t*Boc-Ala-Pro-NHMe,[5] 15% for Ala-Pro,[12] and 13% for Ala-Ala-Pro-Ala[15] in water. This may be due to the different end groups and/or chain lengths of the peptides used in experiments from the Ala-Pro tripeptide.

Prolyl Cis−Trans Isomerization. We located one transition state ts1 of the cis−trans isomerization for each of the Ala-Pro and Aib-Pro peptide bonds in the gas phase and in water, which are both the clockwise rotation through $\omega_1 \approx +120°$ about the prolyl peptide bond but have different backbone conformations, as described above.

At the B2PLYP-D/6-311++G(d,p)//M06-2X/6-31+G(d) level of theory in the gas phase, the rotational barriers ($\Delta G^{\ddagger}_{tc}$ and $\Delta G^{\ddagger}_{ct}$) to the trans-to-cis and cis-to-trans isomerizations are estimated to be 18.02 and 18.76 kcal/mol for the Ala-Pro tripeptide, respectively, and 15.91 and 15.05 kcal/mol for the Aib-Pro tripeptide, respectively (see Tables 1 and 3). At the same level of theory with the SMD method in water, the values of $\Delta G^{\ddagger}_{tc}$ and $\Delta G^{\ddagger}_{ct}$ are calculated to be 20.21 and 19.73 kcal/mol for the Ala-Pro tripeptide, respectively, and 19.67 and 16.64 kcal/mol for the Aib-Pro tripeptide, respectively (see Tables 2 and 4). These calculated results indicate that the rotational barriers $\Delta G^{\ddagger}_{tc}$ and $\Delta G^{\ddagger}_{ct}$ of the Aib-Pro tripeptide become lower by 0.54 and 3.09 kcal/mol than those of the Ala-Pro tripeptide in water, respectively. In addition, the rotational barriers $\Delta G^{\ddagger}_{tc}$ of both the tripeptides increase as the solvent polarity increases, i.e., on going from the gas phase to water, as seen for Ac-Pro-NHMe.[40] In particular, the calculated value of 19.73 kcal/mol for $\Delta G^{\ddagger}_{ct}$ of Ac-Ala-Pro-NHMe in water is consistent with the observed value of 19.3 kcal/mol for Suc-Ala-Ala-Pro-Phe-pNA from NMR experiments at 283 K in a buffered solution.[14]

By the analysis of the contributions to rotational barriers in water, the cis−trans isomerizations of Ala-Pro and Aib-Pro peptide bonds are proven to be entirely enthalpy driven, to which the electronic energies have contributed considerably (Tables 2 and 4), as seen for the Ala dipeptide,[40] Pro dipeptide,[40] and Pro derivatives.[50] This is consistent with the experimental results on proline-containing peptides, kinetically determined as a function of temperature.[51]

The kinetic and spectroscopic results have been interpreted as the evidence that indicates the existence of an intramolecular hydrogen bond between the prolyl nitrogen and the following amide N−H group for the transition state structure, which is capable of catalyzing the prolyl isomerization by up to 260-fold in model peptides.[52] The calculated distances $d(N_{Pro}\cdots H-N_{NHMe})$ between the prolyl nitrogen and the following NHMe group for the transition state ts1 in the gas phase and in water are 2.18 and 2.19 Å for the Ala-Pro tripeptide, respectively, and 2.13 and 2.18 Å for the Aib-Pro tripeptide, respectively, as described above. For both the tripeptides, the distance $d(N_{Pro}\cdots H-N_{NHMe})$ becomes a little longer as the solvent polarity increases. The formation of this intramolecular hydrogen bond between the prolyl nitrogen and the following amide group for the transition state structure has been also seen for the Ala dipeptide,[40] Pro dipeptide,[40,53] and Pro derivatives.[50]

Conclusions

In the gas phase, the most preferred conformation of the Ala-Pro tripeptide is FcBd with a type VIa1 β-turn that has the polyproline II structure for the Ala residue and the 3_{10}-helical structure with the cis prolyl peptide bond and the down puckering for the Pro residue. However, the open conformations FtFu and EtAd are equally most favored in water and are more stabilized by 0.48 and 0.42 kcal/mol in relative free energy than the conformation FcBd in water. In particular, the conformation FtFu has the polyproline II structures for both Ala and Pro residues.

The populations of type VI β-turns for the Ala-Pro tripeptide are decreased from 71% in the gas phase to 21% in water, which is reasonably consistent with IR and NMR experimental results on *t*Boc-Ala-Pro-NHMe, suggesting that the type VI β-turn was found to occur in chlorinated solvents and they were switched into open conformations having no intramolecular hydrogen bonds in water.

For the Aib-Pro tripeptide in the gas phase and in water, the most preferred conformation is AtAu that has a type I β-turn with the α_R-helical structures for both the Aib and Pro residues. The populations of type I β-turns for the Aib-Pro tripeptide are obtained to be 66% both in the gas phase and in water. These calculated results are consistent with observed results that Aib has a strong propensity to form $3_{10}/\alpha$-helical conformations and

type I β-turns in position $i + 1$. In particular, it may rationalize why most of the peptaibiotics containing the Aib-Pro sequence have a regular α-helical conformation at the N- or C-terminus but a α-helical structure with a bend in the middle of the helix.

The cis populations of the X-Pro peptide bond are computed to be 21 and 1% for Ala-Pro and Aib-Pro tripeptides in water. The lower cis population for the Aib-Pro tripeptide is ascribed to the preferential formation of the type I β-turns. The cis−trans isomerizations of the Ala-Pro and Aib-Pro peptide bonds in the gas phase and in water proceed via the clockwise rotation with the different backbone conformations. The rotational barriers to cis-to-trans isomerization are estimated to be 19.73 kcal/mol for the Ala-Pro tripeptide and 16.64 kcal/mol for the Aib-Pro tripeptide in water, which indicates that the rotational barrier becomes lower by ∼3 kcal/mol for the Aib-Pro peptide bond. The calculated rotational barrier of 19.73 kcal/mol for Ac-Ala-Pro-NHMe is consistent with the observed value of 19.3 kcal/mol for Suc-Ala-Ala-Pro-Phe-pNA from NMR experiments in a buffered solution. The pertinent distances between the prolyl nitrogen and the following hydrogen of NHMe group for the transition state structures may indicate that the hydrogen bonds between them can play a role in stabilizing these structures.

Acknowledgment. This work was supported by the grant of the Korean Ministry of Education, Science and Technology (The Regional Core Research Program/Chungbuk BIT Research-Oriented University Consortium).

Supporting Information Available: Tables containing backbone torsion angles, thermodynamic properties, prolyl endocyclic torsion angles, and puckering parameters of Ac-Ala-Pro-NHMe and Ac-Aib-Pro-NHMe optimized at the M06-2X/6-31+G(d) level of theory in the gas phase and at the SMD M06-2X/6-31+G(d) level of theory in water, and figures of representative conformations optimized in the gas phase. This material is available free of charge via the Internet at http://pubs.acs.org.

References and Notes

(1) (a) Lewis, P. N.; Momany, F. A.; Scheraga, H. A. *Biochim. Biophys. Acta* **1973**, *303*, 211. (b) Zimmerman, S. S.; Scheraga, H. A. *Biopolymers* **1977**, *16*, 811. (c) Chou, P. Y.; Fasman, G. D. *J. Mol. Biol.* **1977**, *115*, 135. (d) Rose, G. D.; Gierasch, L. M.; Smith, J. A. *Adv. Protein Chem.* **1985**, *37*, 1. (e) Hutchinson, E. G.; Thornton, J. M. *Protein Sci.* **1994**, *3*, 2207.

(2) (a) Pal, D.; Chakrabarti, P. *J. Mol. Biol.* **1999**, *294*, 271. (b) Stewart, D. E.; Sarkar, A.; Wampler, J. E. *J. Mol. Biol.* **1990**, *214*, 253. (c) Jabs, A.; Weiss, M. S.; Hilgenfeld, R. *J. Mol. Biol.* **1999**, *286*, 291.

(3) (a) Schmid, F. X.; Mayr, L. M.; Mücke, M.; Schönbrunner, E. R. *Adv. Protein Chem.* **1993**, *44*, 25. (b) Balbach, J.; Schmid, F. X. In *Mechanisms of Protein Folding*, 2nd ed.; Pain, R. H., Ed.; Oxford University Press: New York NY, U.S., 2000; *Chapter 8*. (c) Wedemeyer, W. J.; Welker, E.; Scheraga, H. A. *Biochemistry* **2002**, *41*, 14637. (d) Dugave, C.; Demange, L. *Chem. Rev.* **2003**, *103*, 2475.

(4) (a) Li, H.; Oberhauser, A. F.; Redick, S. D.; Carrion-Vazquez, M.; Erickson, H. P.; Fernandez, J. M. *Proc. Natl. Acad. Sci. U. S. A.* **2001**, *98*, 10682. (b) Tchaicheeyan, O. *FASEB J.* **2004**, *18*, 783. (c) Lummis, S. C. R.; Beene, D. L.; Lee, L. W.; Lester, H. A.; Broadhurst, R. W.; Dougherty, D. A. *Nature* **2005**, *438*, 248. (d) Schwartz, T. U.; Schmidt, D.; Brohawn, S. G.; Blobel, G. *Proc. Natl. Acad. Sci. U. S. A.* **2006**, *103*, 6823. (e) Kokalj, S. J.; Gunčar, G.; Štern, I.; Morgan, G.; Rabzelj, S.; Kenig, M.; Staniforth, R. A.; Waltho, J. P.; Žerovnik, E.; Turk, D. *J. Mol. Biol.* **2007**, *366*, 1569. (f) Weininger, U.; Jakob, R. P.; Eckert, B.; Schweimer, K.; Schmid, F. X.; Balbach, J. *Proc. Natl. Acad. Sci. U. S. A.* **2009**, *106*, 12335.

(5) Boussard, G.; Marraud, M. *Biopolymers* **1979**, *18*, 1297.

(6) Aubry, P. A.; Protas, A. J.; Boussard, G.; Marraud, M. *Acta Crystallogr., Sect. B* **1980**, *36*, 2825.

(7) Boussard, G.; Marraud, M. *J. Am. Chem. Soc.* **1985**, *107*, 1825.

(8) Wöhr, T. Ph.D. Thesis, University of Lausanne, 1996.

(9) Némethy, G.; Gibson, K. D.; Palmer, K. A.; Yoon, C. N.; Paterlini, G.; Zagari, A.; Rumsey, S.; Scheraga, H. A. *J. Phys. Chem.* **1992**, *96*, 6472.

(10) Kang, Y. K.; Jhon, J. S.; Han, S. J. *J. Pept. Res.* **1999**, *53*, 30.

(11) Möhle, K.; Gußmann, M.; Hofmann, H.-J. *J. Comput. Chem.* **1997**, *18*, 1415.

(12) Grathwohl, C.; Wüthrich, K. *Biopolymers* **1976**, *15*, 2025.

(13) Grathwohl, C.; Wüthrich, K. *Biopolymers* **1981**, *20*, 2623.

(14) Harrison, R. K.; Stein, R. L. *J. Am. Chem. Soc.* **1992**, *114*, 3464.

(15) Green, J. D. F.; Perham, R. N.; Ullrich, S. J.; Appella, E. *J. Biol. Chem.* **1992**, *267*, 23484.

(16) Reimer, U.; Scherer, G.; Drewello, M.; Kruber, S.; Schutkowski, M.; Fischer, G. *J. Mol. Biol.* **1998**, *279*, 449.

(17) Karle, I. L. *Acc. Chem. Res.* **1999**, *32*, 693.

(18) Toniolo, C.; Crisma, M.; Formaggio, F.; Peggion, C. *Biopolymers* **2001**, *60*, 396.

(19) Degenkolb, T.; Kirschbaum, J.; Brückner, H. *Chem. Biodivers.* **2007**, *4*, 1052.

(20) Aravinda, S.; Shamala, N.; Balaram, P. *Chem. Biodivers.* **2008**, *5*, 1238.

(21) (a) Fox, R. O., Jr.; Richards, F. M. *Nature* **1982**, *300*, 325. (b) Rebuffat, S.; Prigent, Y.; Auvin-guette, C.; Bodo, B. *Eur. J. Biochem.* **1991**, *201*, 661. (c) Snook, C. F.; Woolley, G. A.; Oliva, G.; Pattabhi, V.; Wood, S. P.; Blundell, T. L.; Wallace, B. A. *Structure* **1998**, *6*, 783. (d) Anders, R.; Ohlenschläger, O.; Soskic, V.; Wenschuh, H.; Heise, B.; Brown, L. R. *Eur. J. Biochem.* **2000**, *267*, 1784.

(22) Nagaraj, R.; Shamala, N.; Balaram, P. *J. Am. Chem. Soc.* **1979**, *101*, 16.

(23) Prasad, B. V. V.; Shamala, N.; Nagaraj, R.; Chandrasekaran, R.; Balaram, P. *Biopolymers* **1979**, *18*, 1635.

(24) Rao, C. P.; Nagaraj, R.; Rao, C. N. R.; Balaram, P. *Biochemistry* **1980**, *19*, 425.

(25) Venkatachalapathi, Y. V.; Nair, C. M. K.; Vijayan, M.; Balaram, P. *Biopolymers* **1981**, *20*, 1123.

(26) Poli, M. D.; Moretto, A.; Crisma, M.; Peggion, C.; Formaggio, F.; Kaptein, B.; Broxterman, Q. B.; Toniolo, C. *Chem.—Eur. J.* **2009**, *15*, 8015.

(27) Geßmann, R.; Schiemann, N.; Brückner, H.; Petratos, K. *Acta Crystallogr., Sect. C* **2003**, *59*, o413.

(28) (a) Venkatachalapathi, Y. V.; Balaram, P. *Biopolymers* **1981**, *20*, 1137. (b) Rao, C. P.; Balaram, P. *Biopolymers* **1982**, *21*, 2461. (c) Bosch, R.; Jung, G.; Schmitt, H.; Winter, W. *Biopolymers* **1985**, *24*, 979. (d) Karle, I. L.; Flippen-anderson, J. L.; Uma, K.; Balaram, H.; Balaram, P. *Biopolymers* **1990**, *29*, 1433. (e) Aubry, A.; Bayeul, D.; Brückner, H.; Schiemann, N.; Benedetti, E. *J. Pept. Sci.* **1998**, *4*, 502.

(29) (a) Karle, I. L.; Flippen-anderson, J.; Sukumar, M.; Balaram, P. *Proc. Natl. Acad. Sci. U. S. A.* **1987**, *84*, 5087. (b) Blasio, B. Di.; Pavone, V.; Saviano, M.; Lombardi, A.; Nastri, F.; Pedone, C.; Benedetti, E.; Crisma, M.; Anzolin, M.; Toniolo, C. *J. Am. Chem. Soc.* **1992**, *114*, 6273. (c) Ségalas, I.; Prigent, Y.; Davoust, D.; Bodo, B.; Rebuffat, S. *Biopolymers* **1999**, *50*, 71. (d) Rebuffat, S.; Goulard, C.; Hlimi, S.; Bodo, B. *J. Pept. Sci.* **2000**, *6*, 519.

(30) Kawai, M.; Butsugan, Y. *Biopolymers* **1987**, *26*, 83.

(31) Rai, R.; Aravinda, S.; Kanagarajadurai, K.; Raghothama, S.; Shamala, N.; Balaram, P. *J. Am. Chem. Soc.* **2006**, *128*, 7916.

(32) Compagnon, I.; Oomens, J.; Meijer, G.; von Helden, G. *J. Am. Chem. Soc.* **2006**, *128*, 3592.

(33) (a) Burgess, A. W.; Leach, S. J. *Biopolymers* **1973**, *12*, 2599. (b) Paterson, Y.; Rumsey, S. M.; Benedetti, E.; Némethy, G.; Scheraga, H. A. *J. Am. Chem. Soc.* **1981**, *103*, 2947. (c) Barone, V.; Fraternali, F.; Cristinziano, P. L. *Macromolecules* **1990**, *23*, 2038. (d) Amodeo, P.; Barone, V. *J. Am. Chem. Soc.* **1992**, *114*, 9085. (e) Alemán, C.; Perez, J. J. *Int. J. Quantum Chem.* **1993**, *47*, 231. (f) Alemán, C.; Casanovas, J. *J. Chem. Soc., Perkin Trans. 2* **1994**, 563. (g) Alemán, C. *J. Phys. Chem. B* **1997**, *101*, 5046. (h) Bisetty, K.; Catalan, J. G.; Kruger, H. G.; Perez, J. J. *THEOCHEM* **2005**, *731*, 127. (i) Tran, T. T.; Treutlein, H.; Burgess, A. W. *Protein Eng. Des. Sel.* **2006**, *19*, 401.

(34) Frisch, M. J.; Trucks, G. W.; Schlegel, H. B.; Scuseria, G. E.; Robb, M. A.; Cheeseman, J. R.; Montgomery, J. A., Jr.; Vreven, T.; Kudin, K. N.; Burant, J. C.; Millam, J. M.; Iyengar, S. S.; Tomasi, J.; Barone, V.; Mennucci, B.; Cossi, M.; Scalmani, G.; Rega, N.; Petersson, G. A.; Nakatsuji, H.; Hada, M.; Ehara, M.; Toyota, K.; Fukuda, R.; Hasegawa, J.; Ishida, M.; Nakajima, T.; Honda, Y.; Kitao, O.; Nakai, H.; Klene, M.; Li, X.; Knox, J. E.; Hratchian, H. P.; Cross, J. B.; Bakken, V.; Adamo, C.; Jaramillo, J.; Gomperts, R.; Stratmann, R. E.; Yazyev, O.; Austin, A. J.; Cammi, R.; Pomelli, C.; Ochterski, J. W.; Ayala, P. Y.; Morokuma, K.; Voth, G. A.; Salvador, P.; Dannenberg, J. J.; Zakrzewski, V. G.; Dapprich, S.; Daniels, A. D.; Strain, M. C.; Farkas, O.; Malick, D. K.; Rabuck, A. D.; Raghavachari, K.; Foresman, J. B.; Ortiz, J. V.; Cui, Q.; Baboul, A. G.; Clifford, S.; Cioslowski, J.; Stefanov, B. B.; Liu, G.; Liashenko, A.; Piskorz, P.; Komaromi, I.; Martin, R. L.; Fox, D. J.; Keith, T.; Al-Laham, M. A.; Peng, C. Y.; Nanayakkara, A.; Challacombe, M.; Gill, P. M. W.; Johnson, B.; Chen, W.; Wong, M. W.; Gonzalez, C.; Pople, J. A. *Gaussian 03*, revision D.01; Gaussian, Inc.: Wallingford, CT, U.S., 2004.

(35) Frisch, M. J.; Trucks, G. W.; Schlegel, H. B.; Scuseria, G. E.; Robb, M. A.; Cheeseman, J. R.; Scalmani, G.; Barone, V.; Mennucci, B.; Petersson, G. A.; Nakatsuji, H.; Caricato, M.; Li, X.; Hratchian, H. P.; Izmaylov, A. F.; Bloino, J.; Zheng, G.; Sonnenberg, J. L.; Hada, M.; Ehara, M.; Toyota, K.;

Fukuda, R.; Hasegawa, J.; Ishida, M.; Nakajima, T.; Honda, Y.; Kitao, O.; Nakai, H.; Vreven, T.; Montgomery, J. A., Jr.; Peralta, J. E.; Ogliaro, F.; Bearpark, M.; Heyd, J. J.; Brothers, E.; Kudin, K. N.; Staroverov, V. N.; Kobayashi, R.; Normand, J.; Raghavachari, K.; Rendell, A.; Burant, J. C.; Iyengar, S. S.; Tomasi, J.; Cossi, M.; Rega, N.; Millam, J. M.; Klene, M.; Knox, J. E.; Cross, J. B.; Bakken, V.; Adamo, C.; Jaramillo, J.; Gomperts, R.; Stratmann, R. E.; Yazyev, O.; Austin, A. J.; Cammi, R.; Pomelli, C.; Ochterski, J. W.; Martin, R. L.; Morokuma, K.; Zakrzewski, V. G.; Voth, G. A.; Salvador, P.; Dannenberg, J. J.; Dapprich, S.; Daniels, A. D.; Farkas, O.; Foresman, J. B.; Ortiz, J. V.; Cioslowski, J.; Fox, D. J. *Gaussian 09*, revision A.02; Gaussian, Inc.: Wallingford, CT, U.S., 2009.

(36) Zhao, Y.; Truhlar, D. G. *Theor. Chem. Acc.* **2008**, *120*, 215.

(37) Schwabe, T.; Grimme, S. *Phys. Chem. Chem. Phys.* **2007**, *9*, 3397.

(38) Zimmerman, S. S.; Pottle, M. S.; Némethy, G.; Scheraga, H. A. *Macromolecules* **1977**, *10*, 1.

(39) Altona, C.; Sundaralingam, M. *J. Am. Chem. Soc.* **1972**, *94*, 8205.

(40) Kang, Y. K. *J. Phys. Chem. B* **2006**, *110*, 21338.

(41) Frisch, A.; Dennington, R. D., II; Keith, T. A. *GaussView*, version 3.0; Gaussian, Inc.: Pittsburgh, PA, U.S., 2003.

(42) (a) Gonzalez, C.; Schlegel, H. B. *J. Chem. Phys.* **1989**, *90*, 2154. (b) Gonzalez, C.; Schlegel, H. B. *J. Phys. Chem.* **1990**, *94*, 5523.

(43) Foresman, J. B.; Frisch, A. *Exploring Chemistry with Electronic Structure Methods*, 2nd ed.; Gaussian, Inc.: Pittsburgh, PA, U.S., 1996; *Chapter 8*.

(44) Marenich, A. V.; Cramer, C. J.; Truhlar, D. G. *J. Phys. Chem. B* **2009**, *113*, 6378.

(45) Kang, Y. K.; Byun, B. J. *J. Comput. Chem.* **2010**, *31*, 2915.

(46) Kang, Y. K. *THEOCHEM* **2001**, *546*, 183.

(47) (a) Hehre, W. J.; Radom, L.; Schleyer, P. v. R.; Pople, J. A. *Ab Initio Molecular Orbital Theory*; John Wiley & Sons: New York, NY, U.S., 1986; *Chapter 6*. (b) Frisch, A.; Frisch, M. J.; Clemente, F. R.; Trucks, G. W. *Gaussian 09 User's Reference*; Gaussian, Inc.: Wallingford, CT, U.S., 2009.

(48) Delaney, N. G.; Madison, V. *J. Am. Chem. Soc.* **1982**, *104*, 6635.

(49) Beausoleil, E.; Lubell, W. D. *J. Am. Chem. Soc.* **1996**, *118*, 12902.

(50) (a) Kang, Y. K. *J. Phys. Chem. B* **2002**, *106*, 2074. (b) Song, I. K.; Kang, Y. K. *J. Phys. Chem. B* **2006**, *110*, 1915. (c) Jhon, J. S.; Kang, Y. K. *J. Phys. Chem. B* **2007**, *111*, 3496. (d) Kang, Y. K.; Byun, B. J. *J. Phys. Chem. B* **2007**, *111*, 5377. (e) Kang, Y. K.; Park, H. S. *J. Phys. Chem. B* **2007**, *111*, 12551. (f) Kang, Y. K.; Park, H. S. *Biopolymers* **2009**, *92*, 387.

(51) Stein, R. L. *Adv. Protein Chem.* **1993**, *44*, 1, and references therein.

(52) Cox, C.; Lectka, T. *J. Am. Chem. Soc.* **1998**, *120*, 10660.

(53) Fischer, S.; Dunbrack, R. L., Jr.; Karplus, M. *J. Am. Chem. Soc.* **1994**, *116*, 11931.

JP107200F